

Perchlorinated triarylmethyl radical 99% enriched ^{13}C at the central carbon as EPR spin probe highly sensitive to molecular tumbling

Justin L. Huffman^{†,§}, Martin Poncelet^{†,§}, Whylder Moore[‡], Sandra S. Eaton[‡], Gareth R. Eaton[‡],

Benoit Driesschaert^{†,§,}*

† Department of Pharmaceutical Sciences, West Virginia University, School of Pharmacy, Morgantown, WV, 26506, USA.

§ In Vivo Multifunctional Magnetic Resonance Center, Robert C. Byrd Health Sciences Center, West Virginia University, Morgantown, WV, 26506, USA.

‡Department of Chemistry and Biochemistry, University of Denver, Denver, CO 80210, USA.

KEYWORDS: EPR, trityl, triarylmethyl, viscosity, spectral simulation, tumbling.

Abstract

Soluble stable radicals are used as spin probes and spin labels for *in vitro* and *in vivo* Electron Paramagnetic Resonance (EPR) spectroscopy and imaging applications. We report the synthesis and characterization of a perchlorinated triarylmethyl radical enriched 99% at the central carbon, $^{13}\text{C}_1\text{-PTMTC}$. The anisotropy of the hyperfine splitting with the $^{13}\text{C}_1$ ($A_x=26$, $A_y=25$, $A_z=199.5$ MHz) and the g ($g_x=2.0015$, $g_y=2.0015$, $g_z=2.0040$) are responsible for a strong effect of the radical tumbling rate on the EPR spectrum. The rotational correlation time can be determined by spectral simulation or via the linewidth after calibration. As spin probe $^{13}\text{C}_1\text{-PTMTC}$ can be used to measure media microviscosity with high sensitivity. Bound to a macromolecule as spin label, $^{13}\text{C}_1\text{-PTMTC}$ could be used to study local mobility and molecular interactions.

Introduction

Stable radicals such as nitroxides or triarylmethyls (TAMs or trityls) have been utilized extensively as spin probes and spin labels for *in vitro* and *in vivo* biomedical electron paramagnetic resonance spectroscopy and imaging. Specially designed nitroxides and trityls with spectral sensitivity to various parameters such as oxygen concentration¹, pH²⁻³, thiol concentration³, viscosity⁴, polarity⁵, redox status⁶, or reactive oxygen species (ROS)⁷⁻⁸ have been developed. In a living system, microviscosity is an essential parameter that can modulate the rate of reactions controlled by diffusion. Abnormal microviscosity levels have been reported in many pathologies.⁹ We recently devised a tetrathiatriarylmethyl radical labeled 99% at the central carbon ($^{13}\text{C}_1$), namely, $^{13}\text{C}_1$ -deuterated Finland trityl or $^{13}\text{C}_1$ -**dFT** (Figure 1), whose EPR spectrum is highly sensitive to molecular tumbling and, therefore, to the media microviscosity.¹⁰⁻¹¹ This sensitivity arose from the strong anisotropy of the hyperfine coupling to the $^{13}\text{C}_1$ ($A_x=A_y=17$, $A_z=162$ MHz) that is not entirely averaged out by molecular tumbling, even in low viscosity medium such as water at room temperature. Below a microviscosity of 6 cP, the spectrum of $^{13}\text{C}_1$ -**dFT** is a doublet, and the effect of viscosity is a line broadening (820 mG/cP at X-Band, 9.5 GHz) affecting both lines equally because of the minimal g anisotropy of the probe ($g_x=2.0033$, $g_y=2.0032$, $g_z=2.00275$). We demonstrated that this water-soluble radical could be used *in vitro*, *ex-vivo*, and *in vivo* to measure microviscosity by EPR.¹² Perchlorinated triarylmethyl radicals constitute another class of trityls used in biomedical EPR to measure oxygen *in vivo*¹³⁻¹⁴, detect superoxide¹⁵⁻¹⁶ or hydroxyl radical¹⁷, and as hyperpolarizing agents for dynamic nuclear polarization (DNP)¹⁸⁻¹⁹ or in material sciences.²⁰⁻²¹ A perchlorotriarylmethyl tricarboxylic acid radical (**PTMTC**) 50% enriched $^{13}\text{C}_1$ has been reported recently by Elewa et al.²² The authors showed that the linewidths of the doublet arising from the hyperfine interaction with the $^{13}\text{C}_1$ were also strongly sensitive to viscosity. Moreover, the viscosity-induced line broadening did not affect the two lines equally at X-Band, with a more substantial effect on the low-field peak. However, the characterization of the anisotropy of the hyperfine splitting and g tensor responsible for this spectral sensitivity to the tumbling rate of the radical was not provided, nor the characterization of the tumbling correlation times (τ_R) of the radical with the media microviscosity. We now report the synthesis of a 99% enriched $^{13}\text{C}_1$ -**PTMTC**, its EPR characterization as probe to measure microviscosity and molecular interaction.

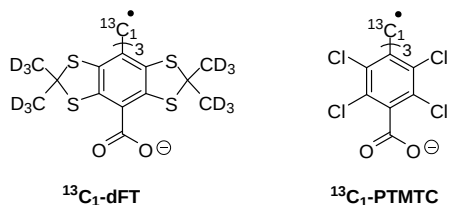


Figure 1. Structure of two $^{13}\text{C}_1$ enriched trityl radicals sensitive to molecular tumbling

Methods

General

NMR spectra were recorded using a Jeol ECZ 400S NMR spectrometer (400 MHz), then processed with MestReNova 14. EPR spectra in water and glycerol/water mixtures were recorded at West Virginia

University using a Bruker ELEXSYS E580 X-band spectrometer and a Magnettech L-band spectrometer (Germany). Immobilized EPR spectra in trehalose/sucrose were recorded at the University of Denver on an Bruker ELEXSYS E580 with X-band and Q-Band capabilities. HRMS data were collected using a Thermo Fisher Scientific Q Exactive Mass Spectrometer with an Electron Spray Ionization (ESI) source. HPLC analyses were performed on a Waters Alliance e2695 separations module, equipped with a 2998 PDA detector. Separations were carried out using a Waters XBridge BEH C18 4.6 mm x 50 mm, 2.5 μ m column at 45°C. All solvents were purchased from Fisher Scientific. All commercially available reagents were used as received without further purification. Tetrahydrofuran was purified on an Inert Pure Solv Solvent Purification system from Innovative Technologies Inc. Chloroform – ^{13}C – 99 atom % was purchased from MilliporeSigma. Glycerol (99.99%) was purchased from Acros Organics. All reactions were carried out under argon in flame-dried glassware and in deoxygenated and anhydrous solvents. Solutions of $^{13}\text{C}_1$ -PTMTC were protected from light.

Synthesis

Tris(2,3,5,6-tetrachlorophenyl)methane- $^{13}\text{C}_1$ (**2**). 1,2,4,5-tetrachlorobenzene (8.06 g, 37.3 mmol, 9 eq.), aluminum (III) chloride (1.66 g, 12.4 mmol, 3 eq.), and chloroform ^{13}C 99% (500 mg, 4.1 mmol, 1 eq.) were added to a sealed pressure vessel and placed in a preheated bath (160°C) for 2 hours. The vessel was removed from the bath, then opened immediately, and 10 mL of both 5M HCl and toluene were added to dissolve the mixture. The aqueous layer was extracted with 25 mL of toluene. Then the organic layer was washed with 10 mL of 1 M HCl (3x). The organic layer was dried over magnesium sulfate, filtered, and the solvent evaporated under reduced pressure, then purified by flash chromatography on silica gel with hexanes to yield 833 mg (30%) of an off-white powder. $^1\text{H-NMR}$ (400 MHz, CDCl_3) δ (ppm): 6.99 (d, J = 124 MHz, 1H, $^{13}\text{C-H}$), 7.65 (s, 3H, Ar-H) $^{13}\text{C-NMR}$ (100 MHz, CDCl_3) δ (ppm): 56.2 (C_1), 130.5 (C-Ar), 132.6 (C-Ar), 133.5 (C-Ar), 133.7 (C-Ar), 134.5 (C-Ar), 138.7 (d, J = 51 MHz, C-Ar). HRMS (ESI): calcd for $[\text{C}_{18}^{13}\text{CH}_4\text{Cl}_{12}\text{-H}]^+$ 657.6259, found 657.6445

Tris(4-methoxycarbonyl-2,3,5,6-tetrachlorophenyl)methane- $^{13}\text{C}_1$ (**3**). The trityl trimer **2** (685 mg, 1.04 mmol, 1 eq.) was dissolved in 68 mL of tetrahydrofuran and 1.56 mL of TMEDA (1.22 g, 10.4 mmol, 10 eq.), then cooled to -78°C. *n*-BuLi (6.51 mL, 10.4 mmol, 10 eq., 1.6 M) was added to the chilled solution and mixed for 1 hour. Methyl chloroformate (804 μL , 10.5 mmol, 10 eq.) was mixed in the solution at -78°C for 10 min, then mixed for 1 hour at room temperature. An additional 80 μL of methyl chloroformate were added and mixed for 1 hour at room temperature. The tetrahydrofuran and TMEDA were evaporated under reduced pressure, then the crude was dissolved in dichloromethane (15 mL). The organic layer was washed with 5 mL of water, 1 M HCl, then water again. The organic layer was dried over magnesium sulfate, filtered, and the solvent evaporated under reduced pressure. The solid was purified by flash chromatography on silica gel using hexanes/ethyl acetate to afford 407 mg (47%) of dark yellow solid. $^1\text{H-NMR}$ (400 MHz, CDCl_3) δ (ppm): 4.01 (s, 9H, COO- CH_3), 7.01 (d, J = 120 MHz, 1H, $^{13}\text{C-H}$) $^{13}\text{C-NMR}$ (100 MHz, CDCl_3) δ (ppm): 53.1 (CH_3), 56.5 (C_1), 129.7 (C-Ar), 130.7 (C-Ar), 134.1 (C-Ar), 135.1 (C-Ar), 135.5 (C-Ar), 138.7 (d, J = 51 MHz, C-Ar), 163.8 (CO). HRMS (ESI): calcd for $[\text{C}_{24}^{13}\text{CH}_{10}\text{Cl}_{12}\text{O}_6\text{-H}]^+$ 831.7339, found 831.6608

Tris(4-methoxycarbonyl-2,3,5,6-tetrachlorophenyl)methyl radical- $^{13}\text{C}_1$ (**4**). To 10 mL of tetrahydrofuran, **3** (115 mg, 0.138 mmol) was added and shielded from light with aluminum foil. Benzyltetramethylammonium hydroxide solution in methanol (40% v/v, 121 μL , 0.276 mmol, 2 eq.) was added and mixed for 1 hour. *p*-chloranil (136 mg, 0.552 mmol, 4 eq.) was added to the solution and mixed

for 3 hours in dark conditions. The solvent was evaporated under reduced pressure, and the red solid was directly purified by flash chromatography on silica gel using hexanes/ethyl acetate to afford 111 mg (97%) of red solid. HRMS (ESI): calcd for $[C_{24}^{13}CH_9Cl_{12}O_6]^+$ 831.7328, found 831.6607

Tris(4-carboxy-2,3,5,6-tetrachlorophenyl)methyl radical- $^{13}C_1$ sodium salt ($[^{13}C_1, 99\%]$ -PTMTC). **4** (139.9 mg, 0.168 mmol) was added to a flask with 17.5 mL of neat, concentrated sulfuric acid, then heated at 90°C for 4 hours. The reaction was cooled to room temperature. Then the mixture was slowly poured over cracked ice. The aqueous layer was extracted with 5 mL of diethyl ether (5x), then the organic layers were dried over magnesium sulfate, filtered, and the solvent evaporated under reduced pressure. Compound $[^{13}C_1, 99\%]$ -PTMTC was purified by reverse phase flash chromatography on C18 silica using 1% trifluoroacetic acid in water/acetonitrile. The red powder containing 70% of $[^{13}C_1, 99\%]$ -PTMTC and 30% of its reduced triarylmethane analog **PTMTC-H** (as determined by HPLC/UV) was freeze-dried, added to water and titrated to pH 6.0 with NaOH, then freeze-dried again to afford 105 mg (58%) of the sodium salt of $[^{13}C_1, 99\%]$ -PTMTC as a red powder. HRMS (ESI): calcd for $[C_{21}^{13}CCl_{12}O_6+H]^-$ 787.6369, found 787.6111

Sample preparation and EPR measurements in aqueous glycerol

Samples of $[^{13}C_1, 99\%]$ -PTMTC were prepared in 0, 12.5, 25, 35, 45, 67.5, 80, 85, 90% glycerol (%V/V) in water (Table S1). Concentrations are based on 70% $[^{13}C_1, 99\%]$ -PTMTC/30% $[^{13}C_1, 99\%]$ -PTMTC-H as determined by HPLC/UV. The final concentration of $[^{13}C_1, 99\%]$ -PTMTC was 400 μ M based on the radical concentration. For the X-Band spectra: gas permeable Teflon tubes (Zeus, Inc., USA) (I.D. 1.14 mm) with a 60 μ m wall thickness were filled with 50 μ L of sample and sealed with Kimble Cha-Seal. The temperature of the sample was maintained at 21.2°C, and oxygen was removed from the sample by a steady flow of nitrogen for 20 minutes using a gas and temperature controller (Noxygen, Germany). Acquisition parameters were as follows: microwave power, 1 mW (except 0.1 mW for 0% glycerol); modulation amplitude, 2 G (except 0.5 G for 0% glycerol, 0.7 G for 12.5% glycerol, 1 G for 25% glycerol, and 1.5 G for 35% glycerol); modulation frequency, 100 kHz; sweep width, 150 G (full spectrum) and 60 G (high- and low-field peaks); sweep time, 81.92 s; conversion time, 40.00 ms; points, 2048; each spectrum was recorded in triplicate. The peak-to-peak linewidth of both the high- and low-field peaks at different viscosities are reported in Figure 5C, Table 2 and Table S2. For the L-Band spectrum, 1 mL of the 400 μ M $[^{13}C_1, 99\%]$ -PTMTC solution in water in a 3 mL Eppendorf was placed in the center of the resonator loop. The solution was bubbled with nitrogen for 30 min before acquisition. L-band acquisition parameters were as follows; modulation amplitude, 0.8 G; modulation frequency, 100 kHz; sweep width, 150 G (full spectrum); sweep time, 60 s; conversion time; points, 2048; non saturating power; room temperature ($\approx 20^\circ$ C).

EPR spectra of $[^{13}C_1, 99\%]$ -PTMTC immobilized in trehalose/sucrose

1.8 mg of solid trityl (70% $[^{13}C_1, 99\%]$ -PTMTC/30% $[^{13}C_1, 99\%]$ -PTMTC-H) was dissolved to 1.0 mL 50 mM PBS pH \sim 7.2. A 2000:1 sugar: radical ratio was selected to give high magnetic dilution. 0.34 g of trehalose and 0.035 g of sucrose were mixed into the trityl solution in a 2.0 mL microfuge tube then shaken and heated gently until a homogenous solution was achieved. The solution was transferred by micropipette to a watch glass, covered by an aluminum foil shell and stored in a desk drawer to protect from light. After 3 days, a pink glass had formed that cracks easily. The glassy solid was placed in a 4 mm OD quartz tube for X-band and a 1.6 mm OD quartz capillary for Q-band. The X-band (9.6196 GHz

spectrum was acquired with a Bruker dielectric resonator, a modulation amplitude of 1.0 G, 100 kHz modulation frequency, and non-saturating microwave power. The Q-band (33.8439 GHz) spectrum was acquired with a Bruker Q-band dielectric resonator, a modulation amplitude of 2.0 G, a modulation frequency of 100 kHz, and a non-saturating microwave power.

Spectral simulation

Spectra were simulated using the Easyspin²³ ver. 5.2.28 and Matlab R2020b. The pepper function of Easyspin was used to fit the rigid spectra, while the chili function was used for the spectra recorded in water and water/glycerol mixtures. All spectra were simulated using $g=[2.0015\ 2.0015\ 2.004]$ and A (MHz)=[26 25 199.5]. The hyperfine splitting in fluid solution was allowed to vary by 2 MHz to account for experimental error and solvent dependence. The calculated hyperfine splittings for the ¹³C satellites (See Table S3) were used as the initial guesses.

Computational chemistry

The geometry of **PTMTC** was optimized at the UB3LYP/6-31G* level of theory using ORCA 4.2.0 computational package.²⁴ The full Cartesian coordinates are given in the supplementary information. The isotropic and anisotropic hyperfine splittings with ¹³C were calculated using the “eprnmr” ORCA keyword for a single point calculation using the IGLO-III basis sets for the optimized geometry.

Interaction with bovine serum albumin

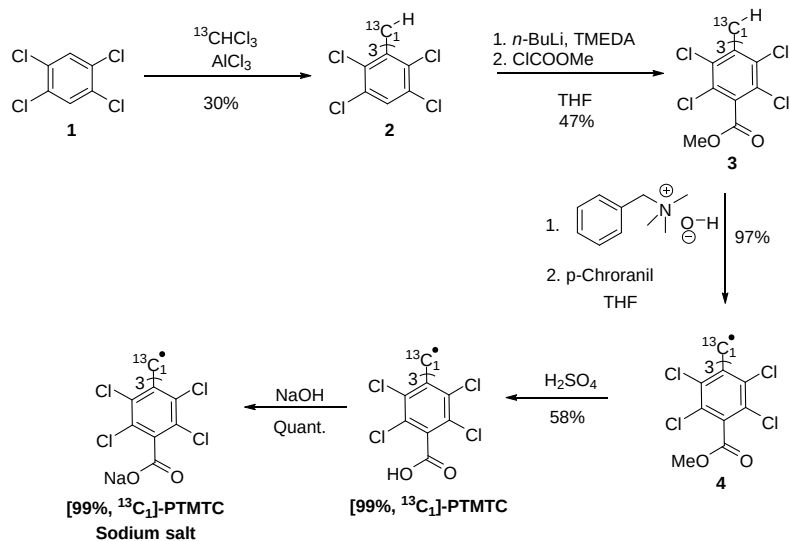
A 1 mM [¹³C₁, 99%]-**PTMTC** in 1 mM aqueous BSA solution was prepared, and the spectrum was recorded at X-Band under nitrogen flow using the following parameters. Microwave power, 1 mW; modulation amplitude, 0.9 G; modulation frequency, 100 kHz; sweep width, 150 G; sweep time, 81.92 s; conversion time, 40.00 ms; points, 2048.

Results and discussions

Elewa et al. reported a 50% enriched ¹³C₁-**PTMTC** which exhibits a doublet EPR spectrum in solution with an isotropic hyperfine coupling to the ¹³C₁ of $A_{\text{iso}} = 83.5$ MHz (29.82 G)²². This value is significantly higher than for the ¹³C₁-**dFT** analog ($A_{\text{iso}} = 65.38$ MHz, 23.35G)¹⁰⁻¹¹ which indicates a higher spin density at the central carbon for **PTMTC** than for the Finland trityl derivative. This larger isotropic hyperfine splitting could lead to a higher spectral sensitivity to the probe tumbling if the anisotropy is proportionately larger for ¹³C₁-**PTMTC** than for ¹³C₁-**dFT**. However, the anisotropic values of the hyperfine interaction were not reported.²² To get insight into the anisotropy of the ¹³C₁ hyperfine interaction, we performed a density functional theory calculation at the B3LYP level using the IGLO-III basis sets, specially tailored for the calculation of EPR properties (Table 1 and SI). The calculated isotropic hyperfine splitting of $A_{\text{iso}}(C_1) = 77.6$ MHz is in good agreement with the experimental value of 83.5 MHz.²² The calculated $A_x=A_y=12.5$ MHz and $A_z=208.0$ MHz for the ¹³C₁ supports a strong anisotropy of the hyperfine interaction and, therefore, high spectral sensitivity to the tumbling rate of the radical. The calculated hyperfine anisotropy $A_{\parallel} - A_{\perp} = 195.5$ MHz, (69 G) is higher than the A anisotropy for the ¹³C₁-**dFT** ($A_{\parallel} - A_{\perp} = 144$ MHz, 52 G).¹¹

To be used as a spin probe that is sensitive to molecular tumbling a ¹³C₁-**PTMTC** with higher than 50% ¹³C enrichment is desirable for maximum signal to noise ratio. Therefore, we synthesized 99% enriched ¹³C₁-**PTMTC** in a four steps sequence as depicted in Scheme 1. The synthetic strategy uses the

procedures reported for **PTMTC** with minimal modifications and the use of a commercially available chloroform- ^{13}C , 99 atom% ^{13}C to label the central carbon with 99% ^{13}C .^{22, 25-26} The sodium salt $^{13}\text{C}_1$ -**PTMTC** was used throughout the study to ensure high aqueous solubility. Since ion pairing is expected to be weak in aqueous solution and the pKa for chlorinated benzoic acids are low, the dominant species in solution is the carboxylate anion.



Scheme 1. Synthesis of [99%, $^{13}\text{C}_1$]-PTMTC

The EPR spectrum of $^{13}\text{C}_1$ -**PTMTC** (400 μM) was recorded at X-Band (9.5 GHz) in deoxygenated water at room temperature (21.2°C) (Figure 2A). The spectrum shows a large doublet arising from the hyperfine interaction with the $^{13}\text{C}_1$ with an A_{iso} of 29.82G (83.5 MHz), in agreement with the previous report. The doublet is asymmetric with a broader low-field peak.²² The peak-to-peak linewidth for the low- and high-field peaks are 1.12 G and 1.06 G. Additional lines corresponding to the ^{13}C satellites for $\text{C}_{3,3}$ and C_2 1.1% natural abundance are also well visible, while the ^{13}C satellites for the $\text{C}_{4,4}$ and C_5 are not resolved. Also, the center of the spectrum features a single line corresponding to the 1% residual $^{12}\text{C}_1$ -**PTMTC**. The low- and high-field peaks linewidths are significantly broader than for the $^{12}\text{C}_1$ -**PTMTC**, which has a peak-to-peak linewidth of ≈ 0.4 G under similar conditions.²² Those spectral features indicate incomplete averaging of the A and g anisotropies by the molecular tumbling in water at room temperature. The same sample recorded at L-Band (1.2 GHz) exhibits a symmetric doublet EPR spectrum in which both linewidths are 1 G (Figure 2B). The lack of asymmetry for the L-Band doublet confirms that an incomplete averaging of the g anisotropy of $^{13}\text{C}_1$ -**PTMTC** is responsible for the asymmetry of the doublet at X-Band.

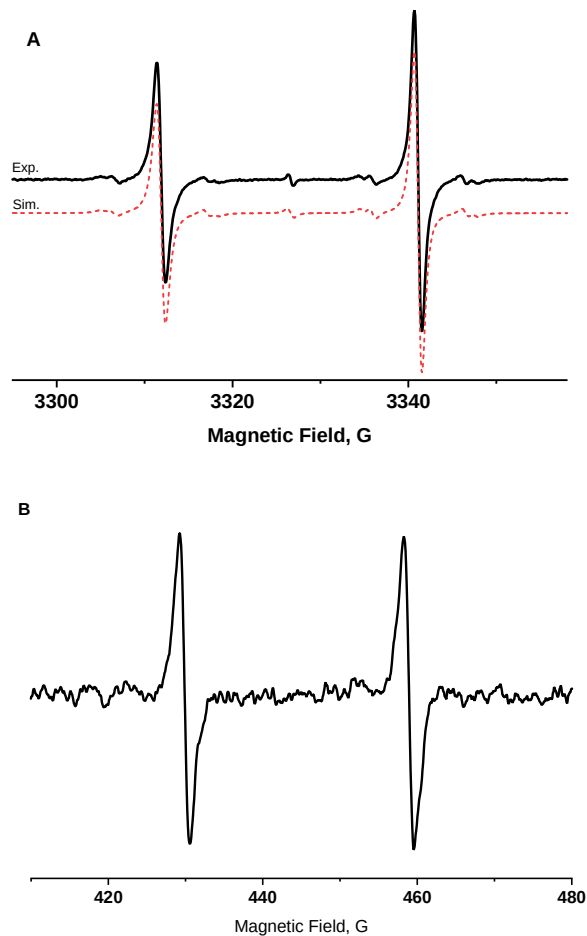


Figure 2. A) X-Band spectrum (in black) of $^{13}\text{C}_1\text{-PTMTC}$ 400 μM in deoxygenated water at room temperature. The spectrum was simulated (in red) using the chili function of EasySpin using the following parameters $g=[2.0015\ 2.0015\ 2.0040]$, A_{C_1} (MHz) = [26 25 199.5], $\text{logtcorr}=-9.73$, 90% contribution. The $\text{C}_{3,3'}$ and C_2 satellites were simulated using additional $A_{\text{C}_{3,3'}}$ (MHz) = [26 26 37], 6% contribution and A_{C_2} (MHz) = [33 33 41], 3% contribution respectively. No hyperfine splittings were used to simulate the 1% contribution of $^{12}\text{C}_1\text{-PTMTC}$. B) L-band spectrum of the same solution.

Next, the $^{13}\text{C}_1\text{-PTMTC}$ was immobilized in 9:1 trehalose: sucrose with a 2000:1 ratio of sugar to radical, and spectra were recorded at room temperature at X-Band (Figure 3A) and Q-Band (Figure 3B). The extrema of the large A_z are well defined at X-Band, which clearly define the value of $g_z=2.0040\pm 0.0002$ and $A_z=199.5\pm 2$ MHz (Table 1). The relatively sharp perpendicular lines require the anisotropy to be small in the x,y-plane. Based on the X-Band spectrum, it was concluded that $A_x=26\pm 2$ MHz, $A_y=25\pm 2$ MHz, and $g_x=g_y=2.0015\pm 0.0002$. The Q-Band spectrum is an unusual case where there is an extensive overlap of the high field A_z line with the perpendicular lines. The spectra at X-Band and Q-Band were simulated using the same A and g values, validating these parameters.

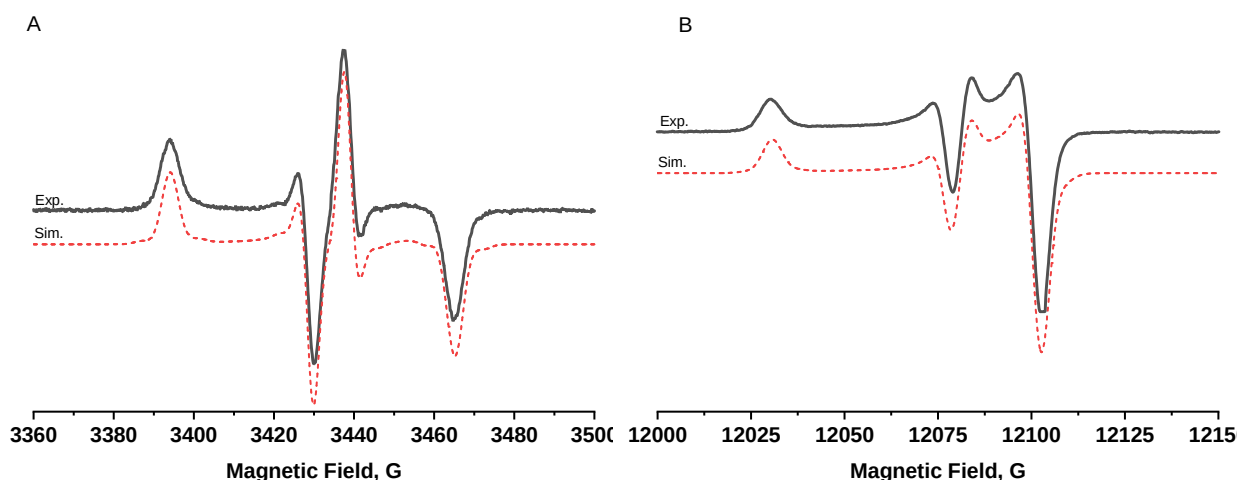


Figure 3. Spectra of $^{13}\text{C}_1\text{-PTMTC}$ at room temperature immobilized in 9:1 trehalose: sucrose with a 2000:1 ratio of sugar to radical. A) The X-Band spectrum (in black) was simulated (in red) using the pepper function of EasySpin using the following parameters $g=[2.0015\ 2.0015\ 2.0040]$, $A\ C_1\ (\text{MHz}) = [26\ 25\ 199.5]$, $H\text{Strain}\ (\text{MHz})=[11.5\ 11.5\ 13.5]$, 91% contribution. The $C_{3,3'}$ and C_2 satellites were simulated using additional $A\ C_{3,3'}\ (\text{MHz}) = [26\ 26\ 37]$, 6% contribution and $A\ C_2(\text{MHz})= [33\ 33\ 41]$, 3% contribution, respectively. B) Q-Band spectrum (in black) was simulated (in red) using the pepper function of EasySpin using the same parameters as the X-band spectrum except $H\text{Strain}\ (\text{MHz})=[16\ 16.5\ 17]$.

Table 1. Experimental and calculated A and g values for $^{13}\text{C}_1\text{-PTMTC}$.

	Experimental ^a	Calculated (MHz) UB3LYP/IGLO-III//UBL3LYP/ 6-31G*
A (MHz)	$A_x=26, A_y=25, A_z=199.5.$ $A_{\text{iso}}=83.5$	$A_x=12.5, A_y=12.5, A_z=208.0$ $A_{\text{iso}}=77.6$
g^b	$g_x=2.0015, g_y= 2.0015,$ $g_z=2.0040\ g_{\text{iso}}=2.0023$	

[a]. In trehalose/sucrose 9:1 at room temperature. [b] Although the differences between g values can be defined with uncertainties of about ± 0.0002 in the simulations, absolute g values have uncertainties of about ± 0.0004 due to the width of lines for radicals used in magnetic field calibrations.

To study the influence of viscosity on the EPR spectra, we prepared solutions of $^{13}\text{C}_1\text{-PTMTC}$ in water/glycerol mixtures and recorded the spectra at X-Band. Figure 4 shows a progressive transition from a relatively narrow doublet at 0% glycerol to a rigid spectrum at 90% glycerol. Above >67.5% glycerol,

26.7 cP, the effect of viscosity on the X-Band spectrum is relatively small with only a slight increase of the apparent A_z from 80% (147.5 cP) glycerol to 90% glycerol (276 cP). Spectral simulation using the chili function of EasySpin allows determination for each solution of the rotational correlation time (τ_R), (Figure 4 and Table 2) which is defined as the time for the molecule to rotate by one radian.

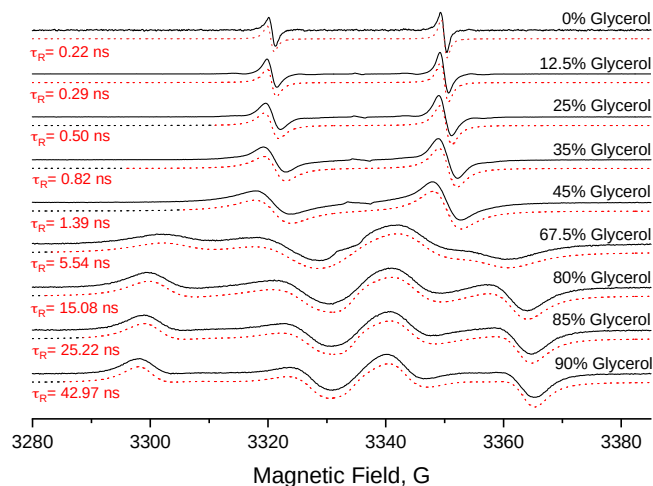


Figure 4. X-Band EPR spectra (in black) of $^{13}\text{C}_1\text{-PTMTC}$ 400 μM in water/glycerol mixtures at 21.2 $^\circ\text{C}$ and simulated spectra (in red) with rotational correlation time (τ_R) determined using the chili function of EasySpin for $g_x=g_y=2.0015$, $g_z=2.0040$, $A_x=26$, $A_y=25$, $A_z=199.5$ MHz.

Table 2. Influence of viscosity on τ_R determined using EasySpin simulations and on the linewidths of the doublet.

Glycerol (%V/V) ^a	Viscosity (cP)	τ_R (ns) ^b	Measured Linewidth	Measured Linewidth
			Low-field peak (G) ^c	High-field peak (G) ^c
0	0.98	0.22±0.04	1.12±0.02	1.06±0.03
12.5	1.46	0.29±0.03	1.66±0.02	1.47±0.02
25	2.34	0.50±0.03	2.56±0.02	2.22±0.02
35	3.62	0.82±0.01	3.84±0.05	3.30±0.04
45	5.99	1.39±0.01	6.05±0.12	4.85±0.12
67.5	26.72	5.54±0.01	-	-
80	84.58	15.08±0.1 9	-	-

85	147.5	25.24±0.9	8	-	-
90	276	42.97±1.7	1	-	-

[a] %V/V Glycerol in deoxygenated water at 21.2°C. [b] Mean of τ_R calculated from three individual spectra. [c] Mean of the peak-to-peak linewidths measured from three spectra.

Figure 5A shows the linear correlation between the τ_R determined by spectral simulations and the media viscosity. It is worth noting that the probe is sensitive to its microenvironment at the submicrometer scale.^{4, 27} The viscosity reported is, therefore, the microviscosity. Because of the lower spectral sensitivity at high viscosity (>30 cP), the accuracy of τ_R determination is decreased for viscosity value >30 cP. The linear fit to τ_R versus viscosity leads to the equation $\tau_R(\text{ns})=0.21 \cdot \text{viscosity}(\text{cP})+0.06$ (for <30 cP). Spectral simulation of the EPR spectrum of $^{13}\text{C}_1\text{-PTMTC}$ offers an accurate way to determine the probe τ_R and media microviscosity.

The Stokes-Einstein equation; $\tau_R = \frac{V\eta}{kT}$ where V is the molecular volume, η is the viscosity, k is the Boltzmann's constant, and T is the temperature, theoretically correlates viscosity to τ_R . A molecular radius of 6.5 Å was estimated based on the optimized geometry of PTMTC at the UB3LYP/6-31G* level of theory (see SI). Using this molar volume, the Stokes-Einstein equation predicts a τ_R of 0.28 ns at 21°C for PTMTC in water (0.98 cP). However, the predictions of the Stokes-Einstein model are better for solute molecules that are much larger than the solvent molecule.²⁸ For smaller molecules, a modified Stokes-Einstein equation; $\tau_R = \frac{V\eta}{kT} C_{\text{slip}}$ with the addition of a slip coefficient (C_{slip}) was suggested to account for deviation from the model.²⁹⁻³⁰ The experimental $\tau_R = 0.22$ ns leads to a $C_{\text{slip}} = 0.78$ which is somewhat larger than the $C_{\text{slip}} = 0.66$ for $^{13}\text{C}_1\text{-dFT}$.¹¹

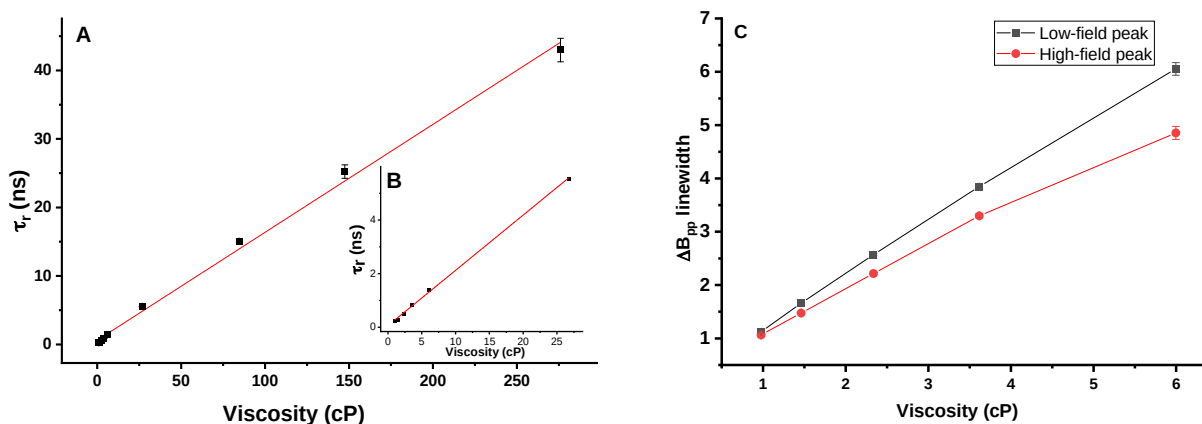


Figure 5. A) τ_R (ns) from spectral simulations versus viscosity (cP). Linear fit leads to the equation $\tau_R(\text{ns})=0.16 \cdot \text{viscosity}(\text{cP})+0.61$, $R^2=0.997$. B) τ_R (ns) versus viscosity (cP) for

viscosity <30 cP, Linear fit leads to the equation $\tau_R(\text{ns})=0.21 \cdot \text{viscosity}(\text{cP})+0.06$, $R^2=0.998$. C) Measured ΔB_{pp} linewidths for the low- and high-field peaks versus viscosity (cP). Linear fit below 4 cP leads to the equations $\Delta B_{pp}(\text{G})=1.03 \cdot \text{viscosity}(\text{cP})+0.14$, $R^2=0.999$ for high-field peak and $\Delta B_{pp}(\text{G})=0.84 \cdot \text{viscosity}(\text{cP})+0.24$, $R^2=1.000$ for the low-field peak.

Below 67.5% of glycerol (26.7 cP), the effect of viscosity on the X-Band spectrum is a line broadening (Figure 4). This broadening is asymmetric between the two peaks because the anisotropy of the g tensor leads to a more substantial effect on the low-field peak (Table 2 and Figure 5B). The linewidths can be calibrated versus τ_R or viscosity as a convenient way to extract those parameters without spectral simulation.¹⁰ For the low-field peak, the linewidth increases linearly with the viscosity for values up to 6 cP, while this relationship deviates from linearity at 4 cP for the high-field peak. The viscosity-induced line broadening of the low-field peak is 1.03G/cP, which is higher than for $^{13}\text{C}_1\text{-dFT}$ (0.82 G/cP)¹⁰. The spectrum of $^{13}\text{C}_1\text{-PTMTC}$ is by consequence, more sensitive to microviscosity and allows for measurement of subtle changes in media microviscosity. Molecular oxygen dissolved in the milieu also results in a broadening of the EPR lines of the probe through the Heisenberg spin exchange. However, the effect of oxygen is minimal by comparison to the viscosity. Indeed, the oxygen-induced line broadening for **PTMTC** is ≈ 0.5 mG/mmHg $p\text{O}_2$ in aqueous samples.²² The maximum broadening due to the presence of dissolved oxygen is therefore ≈ 80 mG ($p\text{O}_2=160$ mmHg or 21%). Thus, oxygen could skew the EPR determined microviscosity by only 0.1 cP, which is minimal. In addition, *in vitro*, the oxygen can easily be displaced inside the EPR cavity, while *in vivo*, the range of $p\text{O}_2$ is even smaller. Simulations have an advantage, relative to calculations based only on changes in linewidths, that contributions to linewidths such as oxygen broadening, concentration dependence or over-modulation of the spectra that impact both hyperfine lines equally can be explicitly taken into account.

PTMTC is an amphiphilic molecule with a lipophilic tetrachlorotriarylmethyl core and three hydrophilic carboxylic acids. Therefore, **PTMTC** is expected to interact with biomacromolecules such as albumin through hydrophobic interactions.³¹ The effect of a decrease of tumbling rate resulting from the interaction with a macromolecule on the EPR spectrum of **PTMTC** is expected to be small because of its single-line spectrum.³¹ $^{13}\text{C}_1\text{-PTMTC}$, on the other hand, is highly sensitive to motion and could find application in studying molecular interactions. To demonstrate the effect of molecular interactions on the EPR spectrum of $^{13}\text{C}_1\text{-PTMTC}$, we prepared a solution of 1 mM $^{13}\text{C}_1\text{-PTMTC}$ in 1mM aqueous bovine serum albumin (BSA), and the spectrum was recorded at X-Band. Figure 6 clearly shows the presence of two spectral components—one sharp doublet (shown with asterisks) corresponding to unbound $^{13}\text{C}_1\text{-PTMTC}$ in fast tumbling, and a more immobilized component (shown with black arrows), corresponding to $^{13}\text{C}_1\text{-PTMTC}$ bound to BSA. Note that a similar interaction with BSA was observed for the Finland trityl.³¹ The correlation time of 38 ns extracted for the $^{13}\text{C}_1\text{-PTMTC}$ bound to BSA is in good agreement with the 30 ns correlation time for BSA measured with a nitroxide probe.³² In comparison, the τ_R predict by the Stokes-Einstein models is 51 ns.³³

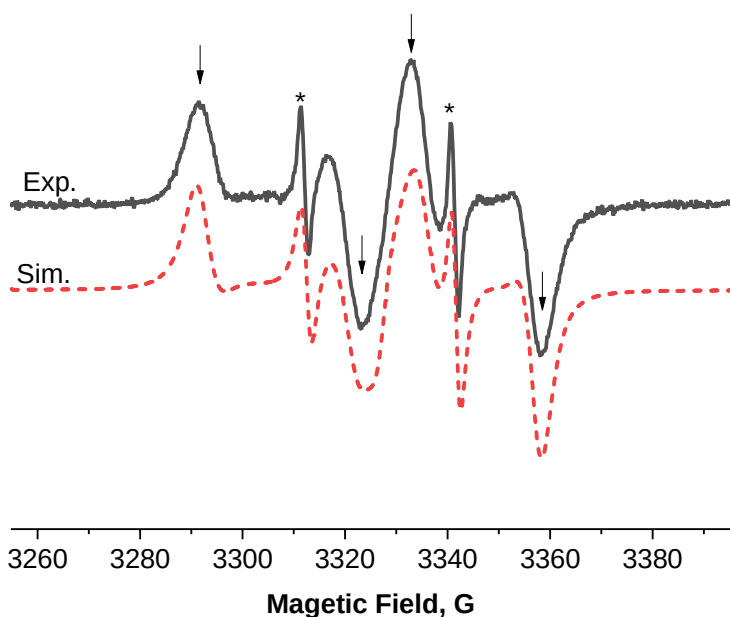


Figure 6. X-Band EPR spectrum (black) of $^{13}\text{C}_1\text{-PTMTC}$ 1 mM in 1mM BSA at room temperature. Simulated spectrum (red) based on two spectral components with $\tau_R=0.30$ ns and $\tau_R=38$ ns.

Conclusion

In conclusion, we have reported the synthesis of a 99% enriched $^{13}\text{C}_1\text{-PTMTC}$ and its EPR characterization. The anisotropy of the A ($A_x=26$, $A_y=25$, $A_z=199.5$ MHz) and the g ($g_x=2.0015$, $g_y=2.0015$, $g_z=2.0040$) are responsible for a strong effect of the radical tumbling rate on the EPR spectrum. The rotational correlation time can be estimated by spectral simulation and used to determine the local microviscosity. Alternatively, the linewidths can be used as an empirical parameter to assess the probe rotational correlation time and microviscosity without spectral simulation. We showed that the change in the EPR spectrum upon interaction with a macromolecule could be used to assess molecular interactions.

Associated Content

The following files are available free of charge. Supporting Information: Sample preparation, NMR, HRMS and HPLC data, cartesian coordinates for **PTMTC**, Experimental and calculated hyperfine splittings.

Author Information

Corresponding author

Benoit Driesschaert

Department of Pharmaceutical Sciences, West Virginia University, School of Pharmacy, Morgantown, WV, 26506, USA; In Vivo Multifunctional Magnetic Resonance Center, Robert C. Byrd Health Sciences Center, West Virginia University, Morgantown, WV, 26506, USA; Phone: + 1 304 293 7401; Email: benoit.driesschaert@hsc.wvu.edu. ORCID: 0000-0002-1402-413X

Authors

Justin L. Huffman

Department of Pharmaceutical Sciences, West Virginia University, School of Pharmacy, Morgantown, WV, 26506, USA; In Vivo Multifunctional Magnetic Resonance Center, Robert C. Byrd Health Sciences Center, West Virginia University, Morgantown, WV, 26506, USA. ORCID: 0000-0003-1835-3501

Martin Poncelet

Department of Pharmaceutical Sciences, West Virginia University, School of Pharmacy, Morgantown, WV, 26506, USA; In Vivo Multifunctional Magnetic Resonance Center, Robert C. Byrd Health Sciences Center, West Virginia University, Morgantown, WV, 26506, USA. ORCID: 0000-0002-2787-8142

Whylder Moore

Department of Chemistry and Biochemistry, University of Denver, Denver, CO 80210, USA. ORCID: 0000-0003-1316-9473

Sandra S. Eaton

Department of Chemistry and Biochemistry, University of Denver, Denver, CO 80210, USA. ORCID: 0000-0002-2731-7986

Gareth R. Eaton

Department of Chemistry and Biochemistry, University of Denver, Denver, CO 80210, USA. ORCID: 0000-0001-7429-8469

Acknowledgments

This work was partially supported by the NIH grants (USA): NIBIB R00 EB023990, NIBIB R21 EB028553 to BD and NCI R01 CA 177744 to GRE and SSE. The content is solely the responsibility of the authors and does not necessarily represent the official views of the NIH.

WVU HSC is acknowledged for start-up funds to B.D. The IMMR center and Prof. Valery. V. Khramtsov are acknowledged for access to the EPR facility. EPR instruments were funded by the NIH grant NIGMS U54 GM104942.

References

1. Serda, M.; Wu, Y.-K.; Barth, E. D.; Halpern, H. J.; Rawal, V. H., EPR Imaging Spin Probe Trityl Radical OX063: A Method for Its Isolation from Animal Effluent, Redox Chemistry of Its Quinone Methide Oxidation Product, and in Vivo Application in a Mouse. *Chem. Res. Toxicol.* **2016**, *29* (12), 2153-2156.
2. Marchand, V.; Levêque, P.; Driesschaert, B.; Marchand-Brynaert, J.; Gallez, B., In vivo EPR extracellular pH-metry in tumors using a triphosphonated trityl radical. *Magn. Reson. Med.* **2017**, *77* (6), 2438-2443.
3. Khramtsov, V. V.; Grigor'ev, I. A.; Foster, M. A.; Lurie, D. J., In vitro and in vivo measurement of pH and thiols by EPR-based techniques. *Antioxid. Redox. Signal.* **2004**, *6* (3), 667-76.
4. Clark, A.; Sedhom, J.; Elajaili, H.; Eaton, G. R.; Eaton, S. S., Dependence of electron paramagnetic resonance spectral lineshapes on molecular tumbling: Nitroxide radical in water:glycerol mixtures. *Concept Magn. Reson. A* **2016**, *45A* (5), e21423.

5. Marsh, D., Spin-Label EPR for Determining Polarity and Proticity in Biomolecular Assemblies: Transmembrane Profiles. *App. Mag. Reson.* **2010**, *37* (1), 435-454.
6. Ilangoan, G.; Li, H.; Zweier, J. L.; Kuppasamy, P., In vivo measurement of tumor redox environment using EPR spectroscopy. *Mol. Cell. Biochem.* **2002**, *234* (1), 393-398.
7. Poncelet, M.; Driesschaert, B.; Bobko, A. A.; Khramtsov, V. V., Triarylmethyl-based biradical as a superoxide probe. *Free Rad. Res.* **2018**, *52* (3), 373-379.
8. Kutala, V. K.; Parinandi, N. L.; Zweier, J. L.; Kuppasamy, P., Reaction of superoxide with trityl radical: implications for the determination of superoxide by spectrophotometry. *Arch. Biochem. Biophys.* **2004**, *424* (1), 81-88.
9. Halpern, H. J.; Chandramouli, G. V. R.; Barth, E. D.; Yu, C.; Peric, M.; Grdina, D. J.; Teicher, B. A., Diminished Aqueous Microviscosity of Tumors in Murine Models Measured with in Vivo Radiofrequency Electron Paramagnetic Resonance. *Cancer Res.* **1999**, *59* (22), 5836-5841.
10. Poncelet, M.; Driesschaert, B., A ¹³C-Labeled Triarylmethyl Radical as an EPR Spin Probe Highly Sensitive to Molecular Tumbling. *Angew. Chem. Int. Ed.* **2020**, *59* (38), 16451-16454.

11. Moore, W.; McPeak, J. E.; Poncelet, M.; Driesschaert, B.; Eaton, S. S.; Eaton, G. R., ¹³C isotope enrichment of the central trityl carbon decreases fluid solution electron spin relaxation times. *J. Magn. Reson.* **2020**, *318*, 106797.
12. Velayutham, M.; Poncelet, M.; Eubank, T. D.; Driesschaert, B.; Khramtsov, V. V., Biological Applications of Electron Paramagnetic Resonance Viscometry Using A ¹³C-labeled Trityl Spin Probe. *Molecules* **2021**, *In revision*.
13. Boś-Liedke, A.; Walawender, M.; Woźniak, A.; Flak, D.; Gapiński, J.; Jurga, S.; Kucińska, M.; Plewiński, A.; Murias, M.; Elewa, M.; Lampp, L.; Imming, P.; Tadyszak, K., EPR Oximetry Sensor—Developing a TAM Derivative for In Vivo Studies. *Cell Biochem. Biophys.* **2018**, *76* (1), 19-28.
14. Bratasz, A.; Kulkarni, A. C.; Kuppusamy, P., A Highly Sensitive Biocompatible Spin Probe for Imaging of Oxygen Concentration in Tissues. *Biophys. J.* **2007**, *92* (8), 2918-2925.
15. Dang, V.; Wang, J.; Feng, S.; Buron, C.; Villamena, F. A.; Wang, P. G.; Kuppusamy, P., Synthesis and characterization of a perchlorotriphenylmethyl (trityl) triester radical: A potential sensor for superoxide and oxygen in biological systems. *Bioorg. Med. Chem. Lett.* **2007**, *17* (14), 4062-4065.

16. Kutala, V. K.; Villamena, F. A.; Ilangovan, G.; Maspoch, D.; Roques, N.; Veciana, J.; Rovira, C.; Kuppusamy, P., Reactivity of Superoxide Anion Radical with a Perchlorotriphenylmethyl (Trityl) Radical. *J. Phys. Chem. B.* **2008**, *112* (1), 158-167.
17. Mesa, J. A.; Chávez, S.; Fajarí, L.; Torres, J. L.; Juliá, L., A tri(potassium sulfonate) derivative of perchlorotriphenylmethyl radical (PTM) as a stable water soluble radical-scavenger of the hydroxyl radical more powerful than 5,5-dimethyl-1-pyrroline-N-oxide. *RSC Adv.* **2013**, *3* (25), 9949-9956.
18. Banerjee, D.; Paniagua, J. C.; Mugnaini, V.; Veciana, J.; Feintuch, A.; Pons, M.; Goldfarb, D., Correlation of the EPR properties of perchlorotriphenylmethyl radicals and their efficiency as DNP polarizers. *Phys. Chem. Chem. Phys.* **2011**, *13* (41), 18626-18637.
19. Paniagua, J. C.; Mugnaini, V.; Gabellieri, C.; Feliz, M.; Roques, N.; Veciana, J.; Pons, M., Polychlorinated trityl radicals for dynamic nuclear polarization: the role of chlorine nuclei. *Phys. Chem. Chem. Phys.* **2010**, *12* (22), 5824-5829.
20. Kimura, S.; Matsuoka, R.; Kimura, S.; Nishihara, H.; Kusamoto, T., Radical-Based Coordination Polymers as a Platform for Magnetoluminescence. *J. Am. Chem. Soc.* **2021**, *143* (15), 5610-5615.
21. Kimura, S.; Uejima, M.; Ota, W.; Sato, T.; Kusaka, S.; Matsuda, R.; Nishihara, H.; Kusamoto, T., An Open-shell, Luminescent, Two-Dimensional Coordination Polymer with a

Honeycomb Lattice and Triangular Organic Radical. *J. Am. Chem. Soc.* **2021**, *143* (11), 4329-4338.

22. Elewa, M.; Maltar-Strmečki, N.; Said, M. M.; El Shihawy, H. A.; El-Sadek, M.; Frank, J.; Drescher, S.; Drescher, M.; Mäder, K.; Hinderberger, D.; Imming, P., Synthesis and EPR-spectroscopic characterization of the perchlorotriarylmethyl tricarboxylic acid radical (PTMTC) and its ¹³C labelled analogue (¹³C-PTMTC). *Phys. Chem. Chem. Phys.* **2017**, *19* (9), 6688-6697.

23. Stoll, S.; Schweiger, A., EasySpin, a comprehensive software package for spectral simulation and analysis in EPR. *J. Magn. Reson.* **2006**, *178* (1), 42-55.

24. Neese, F., Software update: the ORCA program system, version 4.0. *WIREs Comput. Mol. Sci.* **2018**, *8* (1), e1327.

25. Frank, J.; Elewa, M.; M. Said, M.; El Shihawy, H. A.; El-Sadek, M.; Müller, D.; Meister, A.; Hause, G.; Drescher, S.; Metz, H.; Imming, P.; Mäder, K., Synthesis, Characterization, and Nanoencapsulation of Tetrathiatriarylmethyl and Tetrachlorotriarylmethyl (Trityl) Radical Derivatives—A Study To Advance Their Applicability as in Vivo EPR Oxygen Sensors. *J. Org. Chem.* **2015**, *80* (13), 6754-6766.

26. Ballester, M.; Riera, J.; Castañer, J.; Rovira, C.; Armet, O., An Easy, High-yield Synthesis of Highly Chlorinated Mono-, Di- and Triarylmethanes. *Synthesis* **1986**, 1986 (01), 64-66.
27. Morse, P. D.; Luszczakoski, D. M.; Simpson, D. A., Internal microviscosity of red blood cells and hemoglobin-free resealed ghosts: a spin-label study. *Biochem.* **1979**, 18 (22), 5021-5029.
28. Percival, P. W.; Hyde, J. S., Saturation-recovery measurements of the spin-lattice relaxation times of some nitroxides in solution. *J. Magn. Reson.* **1976**, 23 (2), 249-257.
29. D Kivelson, a.; Madden, P. A., Light Scattering Studies of Molecular Liquids. *Annu. Rev. Phys. Chem.* **1980**, 31 (1), 523-558.
30. McClung, R. E. D.; Kivelson, D., ESR Linewidths in Solution. V. Studies of Spin-Rotational Effects Not Described by Rotational Diffusion Theory. *J. Chem. Phys.* **1968**, 49 (8), 3380-3391.
31. Song, Y.; Liu, Y.; Liu, W.; Villamena, F. A.; Zweier, J. L., Characterization of the binding of the Finland trityl radical with bovine serum albumin. *RSC Adv.* **2014**, 4 (88), 47649-47656.

32. Cobb, C. E.; Hustedt, E. J.; Beechem, J. M.; Beth, A. H., Protein rotational dynamics investigated with a dual EPR/optical molecular probe. Spin-labeled eosin. *Biophys. J.* **1993**, *64* (3), 605-613.

33. Gelamo, E. L.; Itri, R.; Alonso, A.; da Silva, J. V.; Tabak, M., Small-angle X-ray scattering and electron paramagnetic resonance study of the interaction of bovine serum albumin with ionic surfactants. *J. Colloid Interface Sci.* **2004**, *277* (2), 471-482.

Table of contents

